

PCCP

Physical Chemistry Chemical Physics

Accepted Manuscript

This article can be cited before page numbers have been issued, to do this please use: X. Cai, G. Sun, Y. Xu, J. Ma and D. Xu, *Phys. Chem. Chem. Phys.*, 2021, DOI: 10.1039/D1CP02759J.



This is an Accepted Manuscript, which has been through the Royal Society of Chemistry peer review process and has been accepted for publication.

Accepted Manuscripts are published online shortly after acceptance, before technical editing, formatting and proof reading. Using this free service, authors can make their results available to the community, in citable form, before we publish the edited article. We will replace this Accepted Manuscript with the edited and formatted Advance Article as soon as it is available.

You can find more information about Accepted Manuscripts in the [Information for Authors](#).

Please note that technical editing may introduce minor changes to the text and/or graphics, which may alter content. The journal's standard [Terms & Conditions](#) and the [Ethical guidelines](#) still apply. In no event shall the Royal Society of Chemistry be held responsible for any errors or omissions in this Accepted Manuscript or any consequences arising from the use of any information it contains.

ARTICLE

Effect of hydrogenation on thermal conductivity of 2D Gallium Nitride

Xueru Cai^a, Guoqing Sun^a, Yaxin Xu^a, Jinlong Ma^a and Dongwei Xu^{a*}Received 00th January 20xx,
Accepted 00th January 20xx

DOI: 10.1039/x0xx00000x

The indirect property of two-dimensional GaN bandgap hinders its application in optical field. Hydrogenation can convert the bandgap of GaN monolayer from an indirect to direct one and also tune the bandgap size. The thermal transport, an important property in the application of two-dimensional material, is also influenced by hydrogenation. By performing first-principle calculation and solving phonon Boltzmann equation, we investigate the effect of hydrogenation on thermal conductivity of GaN monolayer. The results show that hydrogenation will slightly increase the thermal conductivity of GaN monolayer from $70.62 \text{ Wm}^{-1}\text{K}^{-1}$ to $76.23 \text{ Wm}^{-1}\text{K}^{-1}$ at 300K. The little effect of hydrogenation on thermal conductivity is mainly dominated by two competing factors: (1) the reduction of ZA mode lifetime due to the breaking of reflection symmetry after hydrogenation, and (2) the increased contribution from TA and LA modes due to the reduction of anharmonic scattering caused by the enlarged phonon bandgap after hydrogenation. The results are compared with other two-dimensional materials with hexagonal monolayer structures.

Introduction

Gallium Nitride (GaN) has attracted considerable interests for its wide direct bandgap and high carrier mobility[1-3]. Apart from the well-known application in light emitting diodes (LEDs)[1], GaN has also been developed to the fabrication of microwave power transistors[4], solar cell[5] and terahertz detectors[6]. Motivated by the exploration of two-dimensional (2D) materials, 2D GaN, especially GaN monolayer has also attracted much attention[7-16]. Onen et al.[11] systematically investigated GaN from three- to two-dimensional and demonstrated that GaN monolayer has a wider bandgap and a totally different optical spectrum, indicating its application in new optoelectronic application. Nocona et al.[10] further demonstrated its promising potential in nonlinear optics, energy-efficient display application and germicidal and water-purification process.

While possessing above mentioned advantages, GaN monolayer has an indirect electronic bandgap, a critical defect that would largely decrease photoelectric conversion efficiency and hinder its further application in optical-electronic devices[17]. The indirect bandgap mainly comes from surface dangling bonds resulting from the bond breaking when bulk GaN reduces the dimension to 2D[18-20]. Since the polarized covalent bond in GaN play an important role in inducing the dangling bonds at the surface, chemical functionalization provides an effective way to modulate the electronic band by changing the bonding state[21]. Recent research has proved

that hydrogenation can tune GaN monolayer from indirect to direct band and further enlarge the electronic bandgap[9]. The change of bond state by functionalization will also alter the bond strength and then influence the thermal properties[22-30]. However, the effect of chemical functionalization on the thermal conductivity is not universal. For examples, hydrogenation will largely suppress the thermal conductivity of graphene[22, 23] and tetrahexabon[29] while significantly enhance the thermal conductivity of silicene[26] and pentagraphene[25].

Former researches have revealed the anomalously temperature-dependent thermal conductivity and orbit driven low thermal conductivity of GaN monolayer[7, 13]. But the thermal transport in hydrogenated GaN and the effect of hydrogenation remains unknown. In this work, we systematically investigate the thermal transport in hydrogenation GaN monolayer using first-principles calculation. By comparing with GaN monolayer, we demonstrate that hydrogenation only slightly raise the thermal conductivity of GaN monolayer, which are further investigated by mode analysis.

Methods

First-principles calculations are performed using the Vienna ab initio simulation package (VASP) based on density function theory (DFT)[31, 32]. Generalized gradient approximation (GGA) in form of Perdew Burke and Ernzerhod (PBE) is used to describe the exchange correlation functional[33]. The projector-augmented-wave (PAW) potentials are used for Ga and N where the 3d electrons of Ga is described as valence. A vacuum of 20 \AA is set on the out of plane direction to prevent the interaction from neighbouring images. The energy cut for

^a State Key Laboratory of Coal Combustion, School of Energy and Power Engineering, Huazhong University of Science and Technology, Wuhan, Hubei 430074, China.

*correspondence to: dwxu@hust.edu.cn

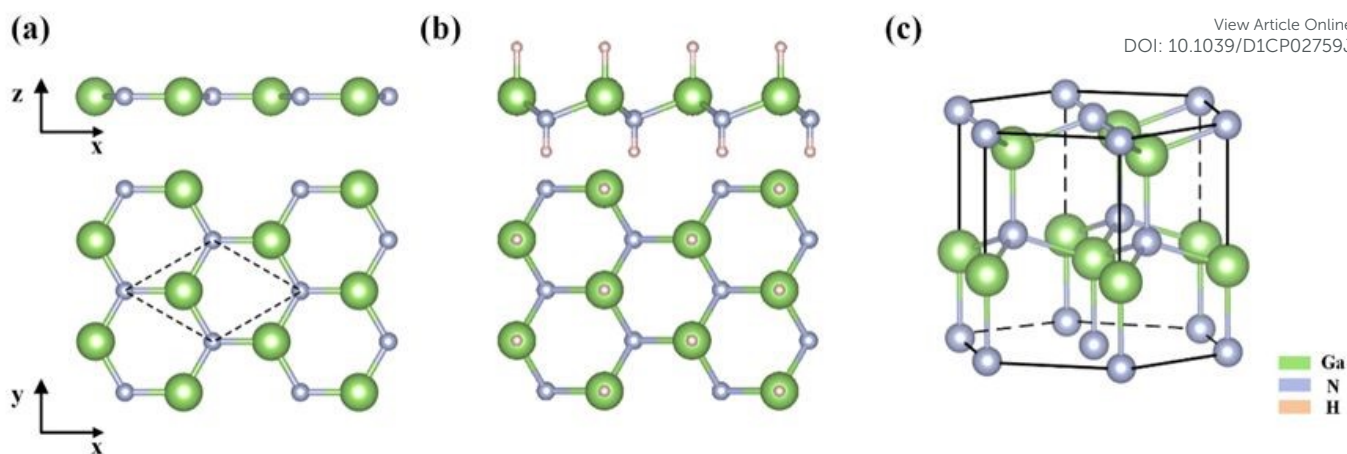


Figure 1. Structure of (a) GaN monolayer; (b) hydrogenated GaN monolayer; (c) bulk GaN

plane wave basis is 900 eV. The convergence criterion for energy and Hellman-Feynman force are set as 10^{-8} eV and 10^{-6} eV/Å respectively. A Gamma-centered $15 \times 15 \times 1$ k-mesh is used to sample the Brillouin zone during structural optimization.

The thermal conductivity is calculated iteratively by solving the phonon Boltzmann using the ShengBTE[34] code. The harmonic force constants (IFCs) are calculated with $5 \times 5 \times 1$ supercell and $2 \times 2 \times 1$ Γ -centered K-mesh using Phonopy[35]. The anharmonic IFCs are calculated with $5 \times 5 \times 1$ supercell using thirdorder[34]. The born effective charge and dielectric constants are also calculated for the correction of long-range electrostatic interaction within density functional perturbation theory (DFPT). A converged cut-off of 5th nearest neighbours and q grid of $130 \times 130 \times 1$ are employed after testing. The thickness of monolayer is chosen as 3.74 Å for both of GaN monolayer and hydrogenated GaN monolayer, which is important in comparing the thermal conductivity of different 2D materials[25, 36].

Results and discussion

optimized structures

The optimized structures of GaN monolayer and hydrogenated GaN monolayer are presented in Fig 1. GaN monolayer exhibits a graphene like planar honeycomb hexagonal structure with the space symmetry group of $P6m2$, which is lower than that of

graphene ($P6/mmm$). The optimized lattice constant is 3.21 Å and the N-Ga bond is 1.85 Å, which is in consistent with previous reports[11, 37]. The planar hexagonal structure comes from sp^2 hybridization due to the dangling bonds when the bulk GaN changes to monolayer. Hydrogenation saturates the missing bonds and restore the 4-coordinated state as in the bulk GaN. After hydrogenation, the space symmetry is degenerated to $P3m1$. The hydrogenated GaN monolayer shows a bulked structure with a buckling height of 0.72 Å. The lattice constants slightly shorten to 3.207 Å while the N-Ga bond is elongated to 1.98 Å.

As an accepted rule of thumb, thermal conductivity is closely related to crystal structure. Complex crystal structure (low space group symmetry) and weak interatomic bonding strength always lead to a lower thermal conductivity. The impact of hydrogenation on thermal conductivity is discussed in the following.

We firstly calculate the thermal conductivity of pristine and hydrogenated GaN monolayer under 300K. The total and relative contributions from different phonon modes are shown in Fig 2(a). At 300K, the thermal conductivity of pristine and hydrogenated GaN monolayer is $70.62 \text{ Wm}^{-1}\text{K}^{-1}$ and $76.23 \text{ Wm}^{-1}\text{K}^{-1}$ respectively. As mentioned above, a more complex crystal structure usually leads to lower thermal conductivity. For example, it has been reported that symmetry-broken would

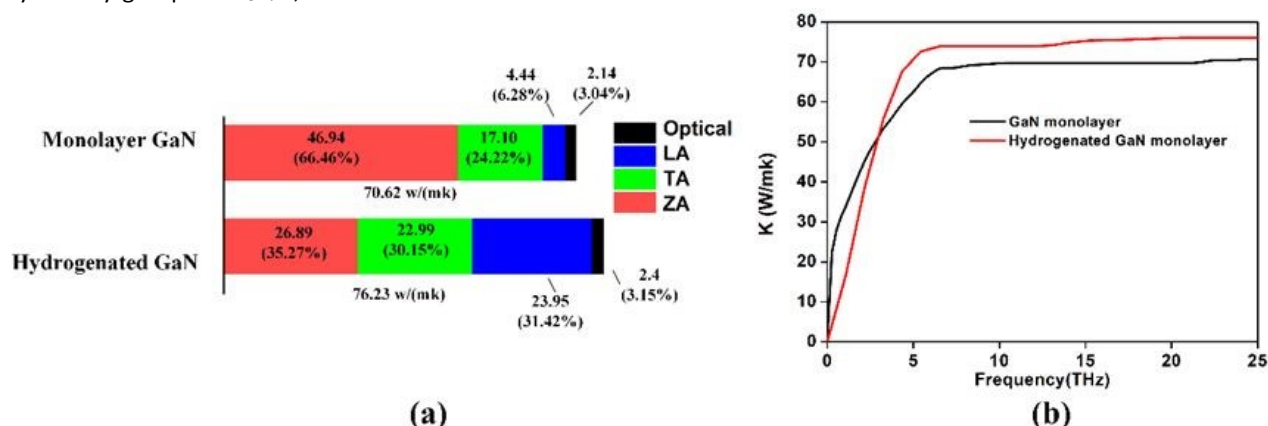


Figure 2. (a) thermal conductivity and relative contribution from different phonon modes of pristine and hydrogenated GaN monolayer; (b) cumulative thermal conductivity as a function of frequency

lead to a planar to bulked structural transition for graphene due to hydrogenation, causing a rapid drop of thermal conductivity from $3590 \text{ Wm}^{-1}\text{K}^{-1}$ to $1328 \text{ Wm}^{-1}\text{K}^{-1}$ [22]. The slightly raised thermal conductivity of hydrogenated GaN monolayer is intriguing here.

To figure out the reasons for the slightly increase of thermal conductivity, we perform a detailed mode analysis. Firstly, we decompose the total thermal conductivity into contributions from different phonon modes as is shown in Fig2(a). For both pristine and hydrogenated GaN monolayer, the main contributions come from acoustic phonon branches, the optical branches only take 3.04% and 3.15% respectively. For pristine GaN monolayer, the ZA (out-of-plane flexural acoustic) mode dominates the thermal conductivity with a contribution of 66.46%. TA (transverse acoustic) and LA (longitudinal acoustic) modes take 24.22% and 6.28% respectively. While hydrogenation has little effect on the apparent thermal conductivity of GaN monolayer, it significantly changes the phonon mode contributions. The contributions from different acoustic branches modes take 35.79%, 30.15% and 31.42% for ZA, TA and LA respectively after hydrogenation. The absolute contribution of ZA modes drops by $20.05 \text{ Wm}^{-1}\text{K}^{-1}$, while the absolute contribution of LA and TA modes increases by $19.55 \text{ Wm}^{-1}\text{K}^{-1}$ and $5.89 \text{ Wm}^{-1}\text{K}^{-1}$ respectively after hydrogenation. The increased contributions of the TA and LA modes compensate

the decrease contribution from ZA mode, and eventually causes the slight increase of total thermal conductivity.

The mode contributions can also be illustrated from frequency dependent thermal conductivity as is shown in Fig 2(b). For both pristine and hydrogenated GaN monolayer, main contributions come from the low frequency phonon under 10 THz. For the pristine GaN, the thermal conductivity from low frequency is especially significant. The cumulative thermal conductivity is already $23 \text{ Wm}^{-1}\text{K}^{-1}$ at 0.3 THz for pristine GaN while it is only $2.5 \text{ Wm}^{-1}\text{K}^{-1}$ at 1 THz for hydrogenated GaN.

phonon dispersion and group velocity

By solving the phonon Boltzmann transport equation (PBTE), the thermal conductivity of crystal can be expressed as:

$$\kappa^{\alpha\beta} = \sum_{\lambda} C_{\lambda} v_{\lambda}^{\alpha} v_{\lambda}^{\beta} \tau_{\lambda}$$

where λ denotes each phonon mode, C_{λ} denotes phonon specific heat, v_{λ} denotes phonon group velocity and τ_{λ} denotes phonon life time. The phonon specific heat for the pristine and hydrogenated GaN is $1.83\text{e}6 \text{ J}/(\text{m}^3\text{K})$ to $2.65\text{e}6 \text{ J}/(\text{m}^3\text{K})$ respectively. Phonon group velocity that can be derived from harmonic term of crystal potential energy is related to harmonic properties. And phonon life time derived from anharmonic terms is denoted the anharmonic properties[38]. Phonon dispersions are shown in Fig 3(a) and Fig3(b) for pristine

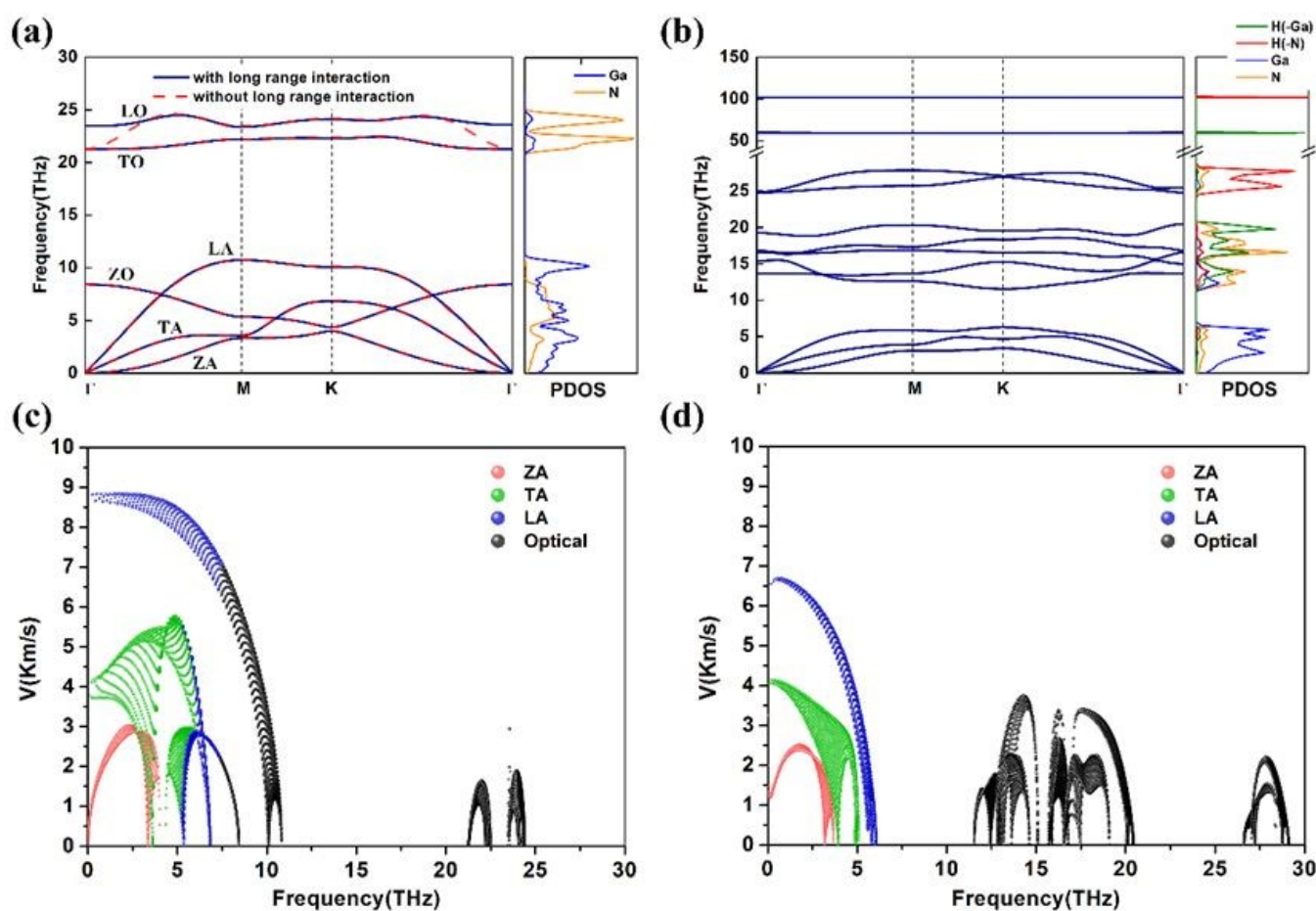


Figure 3. Phonon dispersion and phonon density of state (PDOS) for (a) pristine GaN monolayer; (b) hydrogenated GaN monolayer. Phonon group velocity for (c) pristine GaN monolayer; (d) hydrogenated GaN monolayer

and hydrogenated GaN monolayer respectively. Here, born effect charges and dielectric constants are calculated to consider the long-range Coulomb interaction, which are drawn in blue. As shown in Fig3 (a), long rang interaction mainly effect the high frequency LO modes that are less important to thermal conductivity at room temperature. Both the dispersion curves have no imaginary frequency, indicating the thermal dynamic stability of the materials. It is worthwhile to note that when approaching to Γ points, both ZA modes of hydrogenated and pristine GaN is quadratic, which is consistent with the prediction of 2D continuum elasticity theory[39]. This further demonstrates the accuracy of our results.

From the comparing between Fig3(a) and Fig3(b), hydrogenation changes the phonon frequency distribution significantly. On one hand, hydrogenation suppresses the energy of acoustic phonon as the highest frequency of LA mode dropped from 10THz to 5THz, causing a flatter and more localized phonon dispersion. The localized frequency will produce a considerable impact on the phonon group velocity. On another hand, hydrogenation raises the frequency of ZO mode above the acoustic-optical gap, which suppress the scattering involving ZO mode (such as ZA+ZA->ZO, ZA+TA->ZO, ZA+LA->ZO...). The phonon densities of state (PDOS) are illustrated next to the phonon dispersion in Fig3(a) and Fig3(b). For pristine GaN monolayer, both N and Ga atoms show considerable contribution at lower frequency phonon (<10THz). For hydrogenated GaN monolayer, the PDOS at lower frequency phonon (<5THz) is mainly contributed by Ga atom, while N atom contributes relatively less. The influence of H atom mainly manifests the PDOS at high frequency. The introduction of H atom mainly affects the structure of GaN monolayer and the influence on the thermal transport is due to the change of

structure after hydrogenation. H itself does not contribute directly to thermal conductivity a lot. DOI: 10.1039/D1CP02759J

The group velocity of acoustic phonon branches and optical branch are presented in Fig3(c) and Fig3(d). With the suppression of energy at low frequency, the group velocities of three acoustic phonon branches decrease largely. The maximum group velocity of hydrogenated GaN monolayer are 2.51 km/s (ZA), 4.16 km/s (TA) and 6.70 km/s (LA) respectively, which are lower than those of pristine GaN (3.03km/s (ZA), 5.78 km/s (TA) and 8.48 km/s). The decline of the group velocity has a negative effect on the thermal conductivity and it is hard to make an explanation for the increased contribution of LA modes. To this end, we further calculate the anharmonic properties relating to the variation of mode contribution as discussed below.

Anharmonic properties

The relationships between phonon life time and phonon frequency are shown in Fig4(a) and Fig4(d). For the pristine GaN monolayer, ZA mode has the longest phonon life time, about one order of magnitude larger than TA mode. This is consistent with the largest contribution from ZA modes to thermal conductivity. LA modes have the shortest phonon life time compared with ZA and LA modes, corresponding to the weak contribution to thermal conductivity as shown in Fig1(b). For the hydrogenated GaN monolayer, the phonon life time of LA mode increases sharply by about two order of magnitude, which is even larger than that of ZA modes. The phonon life time of TA mode also increases obviously, especially at low frequency under 5 THz. The increased phonon life time of LA mode clearly explains its raising contribution to thermal conductivity. Moreover, the phonon life time of three different acoustic phonon branches are almost equal, corresponding to a more even contribution to the thermal conductivity from the acoustic

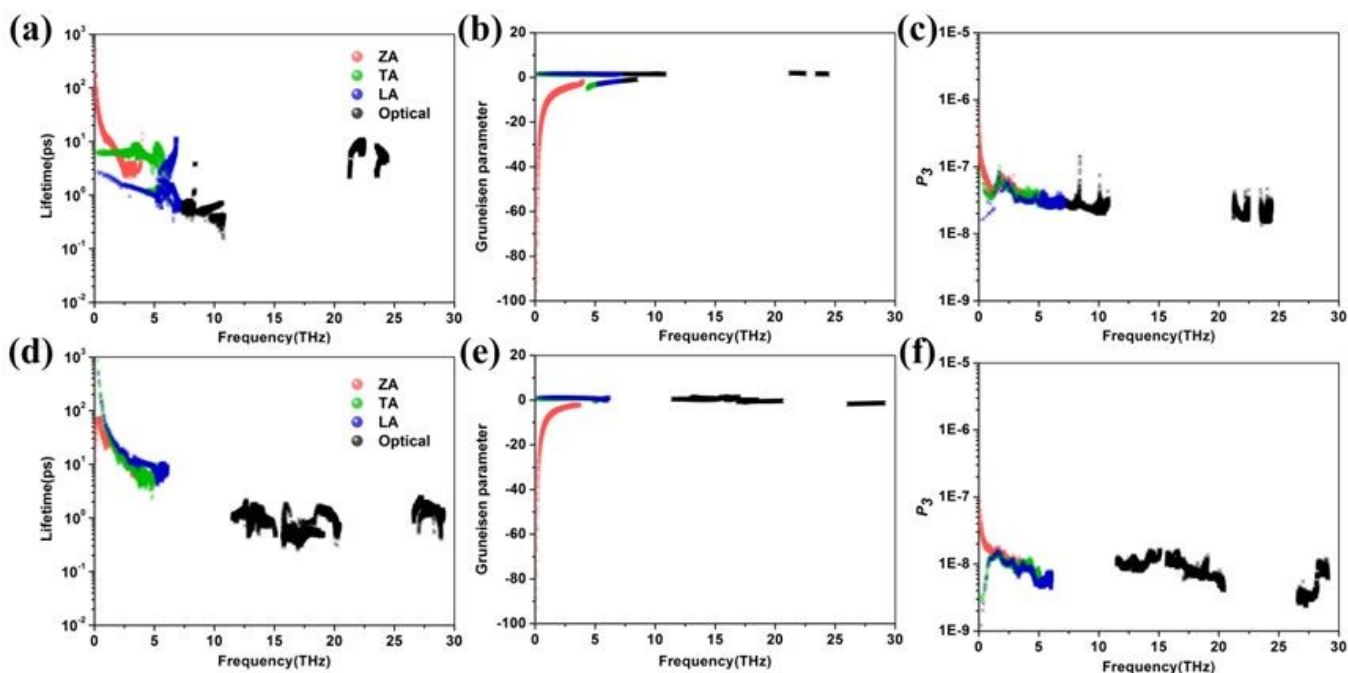


Figure 4. Phonon life time (a)(d), Grüneisen parameters (b)(e) and phonon phase space (c)(f) for pristine (upper panel) and hydrogenated (lower panel) GaN monolayer.

phonon modes. Such a consistency between phonon life time and mode contribution to the thermal conductivity indicates that phonon life time is the determining factor affecting the thermal conductivity of pristine and hydrogenated GaN monolayer.

It is well known that phonon life time mainly depends on two factors. One is the anharmonicity of each scattering channel, and the other is the number of scattering channels[27]. The anharmonicity of scattering channels can be characterized by Grüneisen parameters γ , which is defined as

$$\gamma_{\lambda}(q) = -\frac{A}{\omega_{\lambda}} \frac{\partial \omega_{\lambda}}{\partial A}$$

where A is the area of unit cell and ω_{λ} is the mode dependent phonon frequency. The larger Grüneisen parameters usually mean stronger anharmonicity and lower thermal conductivity. The raise of phonon life time of TA and LA mode can be explained by the decreased phonon anharmonicity as is shown in Fig4(b) and Fig4(e). At 5-10THz, the Grüneisen parameters of

LA and TA mode drop obviously, indicating the decreased phonon anharmonicity of LA and TA mode. DOI: 10.1039/D1CP02759J

We further calculate the phonon phase space (P_3) which can characterize the number of scattering channels, as shown in Fig4(c) and Fig4(f). It is obvious that hydrogenation largely suppresses the P_3 of GaN monolayer. All the P_3 of three acoustic phonon modes decrease about one magnitude.

Fig5 shows the three phonon scattering rate before and after hydrogenation of monolayer GaN. The scattering rate of TA and LA mode decrease significantly, which is consistent with the decreasing phonon phase space and stronger anharmonicity. This can be understood from the phonon dispersion. After hydrogenation, the ZO mode is lifted, reducing the three-phonon scattering channels involving LA, TA and ZO modes. What is abnormal is that the scattering rate of ZA mode increases greatly after hydrogenation. Comparing Fig4(c) and Fig4(f), the possible scattering channels for ZA decreases after hydrogenation. The reason for the increasing scattering rate after hydrogenation is that the buckling structure after hydrogenation breaks the inversion symmetry along z direction[40]. The protected three-phonon scattering involving odd numbers of ZA modes for pristine GaN monolayer is no longer forbidden, causing more ZA modes participating in three phonon scattering and resulting in an even shorter lifetime compared with that of pristine GaN monolayer.

From the above analysis we can see that the main reason causing the change of thermal conductivity after hydrogenation is the structure transformation. We do a search about the relationship of structure and phonon dispersion on two-dimensional hexagonal monolayer materials. The monolayer of BA_s[41], BP[41], SiC[42, 43], BN[44], graphene[45, 46] have the planar hexagonal structures and their corresponding phonon dispersion have overlaps of the ZO mode with the acoustic modes as shown in Fig3(a). After hydrogenation (the same hydrogenated style as discussed in our paper), all the planar structures become buckling, resulting in a lifted ZO modes as shown in Fig3(b). At Γ point, ZO mode corresponds to opposite vibration of two neighbour atoms. After hydrogenation, this vibration modes become harder to be excited. The existence of acoustic-optical gap reduces the three-phonon scattering involving LA, TA and ZO modes, resulting in an increasing of thermal conductivity. However, the buckling structures also broke the inversion symmetry which increases the three phonon scattering rate involving odd number of ZA modes. The structure and phonon dispersion show similar relationships of those two-dimensional hexagonal monolayer before and after hydrogenation, however, the thermal conductivities do not give the same trend since there are at least two competing factors.

Conclusion

By performing first principle calculation and solving PBTE, we systematically investigate the thermal conductivity and detailed phonon transport of hydrogenated and pristine GaN monolayer. Hydrogenation would slightly raise the thermal conductivity of GaN monolayer, which could be attributed to

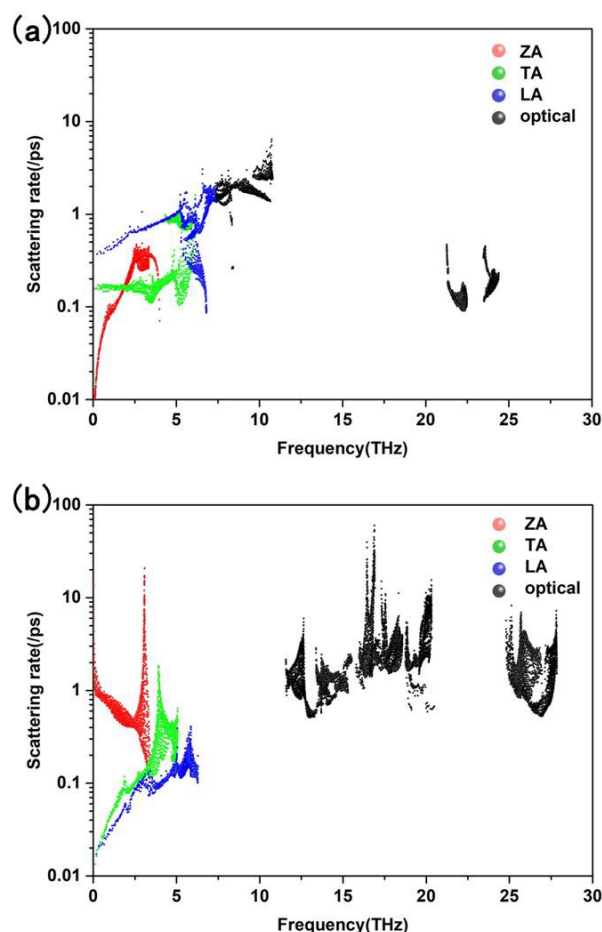


Figure 5. Three phonon scattering rate of the pristine (a) and hydrogenation (b) GaN monolayer.

the coupling effect of decreased ZA modes' contribution and increased LA and TA modes' contribution. The anharmonic properties dominate the thermal conductivity. The phonon life time decreases for the ZA mode due to the symmetry broken after hydrogenation. The increased contribution of LA and TA modes can be attribute to the increase of phonon life time due to the decreasing scattering channels after hydrogenation. The relationship between structure and phonon dispersion of other two-dimensional hexagonal monolayer materials show similar trend: ZO mode overlapping with acoustic modes for planar hexagonal structure and an acoustic-optical gaps arising for the buckling structure after hydrogenation.

Conflicts of interest

There are no conflicts of interest to declare.

Acknowledgement

D.X. acknowledges support from National Natural Science Foundation of China (No. 51806072). J.M. acknowledges support from National Natural Science Foundation of China (No. 11804229).

Notes and references

- Nakamura, S. and M.R. Krames, *History of Gallium-Nitride-Based Light-Emitting Diodes for Illumination*. Proceedings of the IEEE, 2013. **101**(10): p. 2211-2220.
- DenBaars, S.P., et al., *Development of gallium-nitride-based light-emitting diodes (LEDs) and laser diodes for energy-efficient lighting and displays*. Acta Materialia, 2013. **61**(3): p. 945-951.
- Chen, Y.X., et al., *GaN in different dimensionalities: Properties, synthesis, and applications*. Materials Science & Engineering R-Reports, 2019. **138**: p. 60-84.
- Ganguly, S., et al., *Polarization effects on gate leakage in InAlN/AlN/GaN high-electron-mobility transistors*. Applied Physics Letters, 2012. **101**(25): p. 5.
- Neufeld, C.J., et al., *High quantum efficiency InGaN/GaN solar cells with 2.95 eV band gap*. Applied Physics Letters, 2008. **93**(14): p. 3.
- Hou, H.W., et al., *High Temperature Terahertz Detectors Realized by a GaN High Electron Mobility Transistor*. Scientific Reports, 2017. **7**: p. 6.
- Qin, G., et al., *Anomalous temperature-dependent thermal conductivity of monolayer GaN with large deviations from the traditional 1/T law*. Physical Review B, 2017. **95**(19).
- Mu, Y.W., *Chemical Functionalization of GaN Mono layer by Adatom Adsorption*. Journal of Physical Chemistry C, 2015. **119**(36): p. 20911-20916.
- Shu, H., et al., *Effects of strain and surface modification on stability, electronic and optical properties of GaN monolayer*. Applied Surface Science, 2019. **479**: p. 475-481.
- Sanders, N., et al., *Electronic and Optical Properties of Two-Dimensional GaN from First-Principles*. Nano Letters, 2017. **17**(12): p. 7345-7349.
- Onen, A., et al., *GaN: From three- to two-dimensional single-layer crystal and its multilayer van der Waals solids*. 2016. **93**(8).
- Chen, Y.X., et al., *Growth of 2D GaN Single Crystals on Liquid Metals*. Journal of the American Chemical Society, 2018. **140**(48): p. 16392-16395. DOI: 10.1039/D1CP02759J
- Qin, Z.Z., et al., *Orbitally driven low thermal conductivity of monolayer gallium nitride (GaN) with planar honeycomb structure: a comparative study*. Nanoscale, 2017. **9**(12): p. 4295-4309.
- Jiang, Y., *Phonon transport properties of bulk and monolayer GaN from first-principles calculations*. Computational Materials Science, 2017.
- Zhang, J., *Piezoelectric effect on the thermal conductivity of monolayer gallium nitride*. Journal of Applied Physics, 2018. **123**(3): p. 8.
- Al Balushi, Z.Y., et al., *Two-dimensional gallium nitride realized via graphene encapsulation*. Nature Materials, 2016. **15**(11): p. 1166-1173.
- Kittel, C.J.A.J.o.P., *Introduction to Solid State Physics*. 1996. **21**(8).
- Landmann, M., et al., *GaN m-plane: Atomic structure, surface bands, and optical response*. Physical Review B, 2015. **91**(3): p. 8.
- Franz, M., et al., *Valence band structure and effective masses of GaN(10 $\bar{1}$ 0)*. Physical Review B, 2019. **99**(19): p. 6.
- Cai, X., et al., *Structure and electronic bandgap tunability of m-plane GaN multilayers*. Phys Chem Chem Phys, 2021. **23**(9): p. 5431-5437.
- Guo, Y., et al., *Surface chemical-modification for engineering the intrinsic physical properties of inorganic two-dimensional nanomaterials*. Chemical Society Reviews, 2015. **44**(3): p. 637-646.
- Barbarino, G., C. Melis, and L. Colombo, *Effect of hydrogenation on graphene thermal transport*. Carbon, 2014. **80**: p. 167-173.
- Sofo, J.O., A.S. Chaudhari, and G.D. Barber, *Graphane: A two-dimensional hydrocarbon*. Physical Review B, 2007. **75**(15): p. 4.
- Li, T.W., G. Nie, and Q. Sun, *Highly sensitive tuning of lattice thermal conductivity of graphene-like borophene by fluorination and chlorination*. Nano Research, 2020. **13**(4): p. 1171-1177.
- Wu, X., et al., *Hydrogenation of Penta-Graphene Leads to Unexpected Large Improvement in Thermal Conductivity*. 2016. **16**(6): p. 3925-3935.
- Liu, Z.Y., X.F. Wu, and T.F. Luo, *The impact of hydrogenation on the thermal transport of silicene*. 2d Materials, 2017. **4**(2): p. 11.
- Peng, B., et al., *Tuning Thermal Transport in C3N Monolayers by Adding and Removing Carbon Atoms*. Physical Review Applied, 2018. **10**(3).
- Li, T., et al., *The ultralow thermal conductivity and ultrahigh thermoelectric performance of fluorinated Sn2Bi sheet in room temperature*. Nano Energy, 2019: p. 104283.
- Kilic, M.E. and K.R. Lee, *Tuning the electronic, mechanical, thermal, and optical properties of tetrahexcarbon via hydrogenation*. Carbon, 2020. **161**: p. 71-82.
- Peng, B., et al., *First-Principles Prediction of Ultralow Lattice Thermal Conductivity of Dumbbell Silicene: A Comparison with Low-Buckled Silicene*. Acs Applied Materials & Interfaces, 2016. **8**(32): p. 20977-20985.
- Kresse, G. and J. Furthmuller, *Efficient iterative schemes for ab initio total-energy calculations using a plane-wave basis set*. Physical Review B, 1996. **54**(16): p. 11169-11186.
- Kresse, G. and J. Furthmuller, *Efficiency of ab-initio total energy calculations for metals and semiconductors using a plane-wave basis set*. Computational Materials Science, 1996. **6**(1): p. 15-50.
- Perdew, J.P., K. Burke, and M. Ernzerhof, *Generalized gradient approximation made simple*. Physical Review Letters, 1996. **77**(18): p. 3865-3868.
- Li, W., et al., *ShengBTE: A solver of the Boltzmann transport equation for phonons*. Computer Physics Communications, 2014. **185**(6): p. 1747-1758.

35. Togo, A., F. Oba, and I. Tanaka, *First-principles calculations of the ferroelastic transition between rutile-type and CaCl₂-type SiO₂ at high pressures*. *Physical Review B*, 2008. **78**(13): p. 9.
36. Wu, X.F., et al., *How to characterize thermal transport capability of 2D materials fairly? - Sheet thermal conductance and the choice of thickness*. *Chemical Physics Letters*, 2017. **669**: p. 233-237.
37. Xu, D., et al., *Stacking and electric field effects in atomically thin layers of GaN*. 2013. **25**(34): p. 345302.
38. Hua Bao, J.C., XiaoKun Gu and Bingyang Cao, *A review of Simulation Methods in Micro/Nanoscale Heat Conduction* 2018.
39. Liu, D., A.G. Every, and D. Tomanek, *Continuum approach for long-wavelength acoustic phonons in quasi-two-dimensional structures*. *Physical Review B*, 2016. **94**(16): p. 9.
40. Lindsay, L., D.A. Broido, and N. Mingo, *Flexural phonons and thermal transport in graphene*. *Physical Review B*, 2010. **82**(11).
41. Ullah, S., P.A. Denis, and F. Sato, *Hydrogenation and Fluorination of 2D Boron Phosphide and Boron Arsenide: A Density Functional Theory Investigation*. *ACS Omega*, 2018. **3**(12): p. 16416-16423.
42. Chen, X., et al., *Tunable electronic structure and enhanced optical properties in quasi-metallic hydrogenated/fluorinated SiC heterobilayer*. *Journal of Materials Chemistry C*, 2016. **4**(31): p. 7406-7414.
43. Wang, X.-Q. and J.-T. Wang, *Structural stabilities and electronic properties of fully hydrogenated SiC sheet*. *Physics Letters A*, 2011. **375**(27): p. 2676-2679.
44. Kroes, J.M., A. Fasolino, and M.I. Katsnelson, *Energetics, barriers and vibrational spectra of partially and fully hydrogenated hexagonal boron nitride*. *Phys Chem Chem Phys*, 2016. **18**(28): p. 19359-67.
45. Cadelano, E., et al., *Elastic properties of hydrogenated graphene*. *Physical Review B*, 2010. **82**(23).
46. Khatami, M.M., et al., *Electronic transport properties of hydrogenated and fluorinated graphene: a computational study*. *J Phys Condens Matter*, 2020. **32**(49): p. 495502.

View Article Online
DOI: 10.1039/D1CP02759J